



HAL
open science

The Lemaître–Hubble diagram in axial Bianchi IX universes with comoving dust

Galliano Valent, André Tilquin, Thomas Schücker

► **To cite this version:**

Galliano Valent, André Tilquin, Thomas Schücker. The Lemaître–Hubble diagram in axial Bianchi IX universes with comoving dust. *Classical and Quantum Gravity*, 2023, 41 (1), pp.015034. 10.1088/1361-6382/ad13c1 . hal-04355030

HAL Id: hal-04355030

<https://hal.science/hal-04355030>

Submitted on 20 Dec 2023

HAL is a multi-disciplinary open access archive for the deposit and dissemination of scientific research documents, whether they are published or not. The documents may come from teaching and research institutions in France or abroad, or from public or private research centers.

L'archive ouverte pluridisciplinaire **HAL**, est destinée au dépôt et à la diffusion de documents scientifiques de niveau recherche, publiés ou non, émanant des établissements d'enseignement et de recherche français ou étrangers, des laboratoires publics ou privés.

The Lemaître-Hubble diagram in axial Bianchi IX universes with comoving dust

Galliano Valent¹, André Tilquin², Thomas Schücker³

Abstract

Axial Bianchi IX universes have compact, simply connected, homogeneous three-spaces and feature minimal symmetry breaking of the cosmological principle. We consider a positive cosmological constant, comoving dust and a mildly anisotropic expansion in the recent past, $z < 6$, which might be observable in the near future with the James Webb Space Telescope and the Vera Rubin Observatory. To this end we compute the direction dependent redshift and apparent luminosity of type 1a supernovae.

To the memory of Vaughan Jones

PACS: 98.80.Es, 98.80.Cq

Key-Words: cosmological parameters, supernovae, anisotropies

¹Aix Marseille Univ, Université de Toulon, CNRS, CPT, IPhU, Marseille, France;
on leave from LPMP, Aix-en-Provence, France
galliano.valent@orange.fr

²Aix Marseille Univ, CNRS/IN2P3, CPPM, IPhU, Marseille, France
tilquin@cprm.in2p3.fr

³Aix Marseille Univ, Université de Toulon, CNRS, CPT, IPhU, Marseille, France
thomas.schucker@gmail.com

1 Introduction

Bianchi I universes have a long history in cosmology. As early as 1933, Georges Lemaître (1933), following a recommendation by Albert Einstein, considers Bianchi I universes without using this name. The entire Bianchi family (Bianchi 1898) of universes is introduced to cosmology in the late sixties (Ellis & MacCallum 1969; Hawking 1969; Collins & Hawking 1973). These universes are characterized by homogeneous 3-spaces of simultaneity with three Killing vectors. In Bianchi I, the Abelian model in the Bianchi family, the Killing vectors commute. The maximal number of Killing vectors of a 3-space is six. A theorem by Guido Fubini (1903) is central in our work.

Theorem: Consider a Riemannian manifold of dimension $d \geq 3$. Its isometry group cannot be of dimension $n = d(d + 1)/2 - 1$.

It tells us that the sub-maximal number of Killing vectors in 3-space is four. Nevertheless the corresponding universes are contained in Bianchi's classification as special cases, let us call them *axial* Bianchi universes. Some authors, e.g. King & Ellis (1973), use the adjective 'locally rotationally symmetric (L.R.S.)' instead of axial.

For example, the Bianchi I universes have three independent scale factors, $a(t)$, $b(t)$, $c(t)$,

$$d\tau^2 = dt^2 - a(t)^2 dx^2 - b(t) dy^2 - c(t)^2 dz^2, \quad (1)$$

with the three Killing vectors, ∂_x , ∂_y , ∂_z , generating the three translations. Axial Bianchi I universes, $a = b$, have sub-maximally symmetric 3-spaces, and their fourth Killing vector, $x\partial_y - y\partial_x$, generates rotations around the z -axis. Note that in the limit of small anisotropies $(c - a)/a \rightarrow 0$ the axial Bianchi I universes converge to the maximally symmetric flat Robertson-Walker universes.

There are only two more families of universes with the above two properties: (*i*) being sub-maximally symmetric (Fubini 1903) and (*ii*) admitting convergent limits of small anisotropies to universes complying with the cosmological principle. Besides the axial Bianchi I universes these two families are the axial Bianchi V universes (negative curvature) and the axial Bianchi IX universes (positive curvature). The 3-spaces of the latter are also known as Berger spheres (Berger 1961).

The Cosmic Microwave Background data shows small, but significant anisotropies of the order of 10^{-5} motivating property (*ii*). All Bianchi universes close to Robertson-Walker universes, have been used to try and decipher a 3-dimensional subgroup of the 6-dimensional isometry groups in these data. We recommend the reader-friendly overview on this topic by Pereira & Pitrou (2019).

Besides via observation of the Cosmic Microwave Background, deviations from the cosmological principle may also be observed via drifts of extra-galactic sources (Darling 2014; Marcori et al. 2018), via privileged directions in the Lemaître-Hubble diagram of type 1a supernovae (Kolatt & Lahav 2001) and of quasars and gamma-ray bursts (Secrest et al. 2021; Luongo et al. 2022), via weak lensing data (Pitrou, Pereira & Uzan 2015), via galaxy cluster scaling relations (Migkas et al. 2021), via radio galaxies (Siewert, Schmidt-Rubart & Schwarz 2021) and perhaps via black hole or neutron star mergers in the future (Pitrou, Cusin & Uzan 2020).

We mention four recent model-independent analyses of type 1a supernovae, $z < 2.26$, with respect to anisotropies: Rahman et al. (2002), Deng & Wei (2018), Zhao, Zhou & Chang (2019) and Perivolaropoulos (2023). All four find no significant deviations from isotropy. This is mainly due to the inhomogeneous distribution of the observed supernovae in the sky.

Our interest in the Lemaître-Hubble diagram for supernovae is motivated by an expected experimental break-through:

In 2024 the Vera Rubin Observatory (previously referred to as the Large Synoptic Survey Telescope, LSST) should start operating and observe 50 000 supernovae per year up to redshift $z = 1$, improving the precision of the Lemaître-Hubble diagram by one to two orders of magnitude (Schücker, Tilquin & Valent 2014). Complementarily, the James Webb Space Telescope is expected to observe some 200 type 1a supernovae up to redshift $z = 6$ in the next six years (Lu et al. 2022). Also the Chinese Space Station Telescope should start operating in 2024 and observe some 1800 type 1a supernovae below a redshift of $z = 1.3$ in a time span of two years (Li et al. 2023).

So far only Bianchi I universes have been used to fit the Lemaître-Hubble diagram (Saunders 1969; Koivisto & Mota 2008a,b; Campanelli et al. 2011; Schücker et al. 2014; Fleury, Pitrou & Uzan 2015) and the expected break-through encourages us to go beyond the Abelian model.

Computing the Lemaître-Hubble diagram one commonly admits Einstein’s equations with a cosmological constant. One further assumes that radiation can be neglected and that galaxies, supernovae and dark matter are modeled by comoving dust. ‘Comoving’ means that there is a system of coordinates with respect to which the energy-momentum tensor has vanishing time-space components and ‘dust’ means that the space-space components vanish. With these assumptions Farnsworth (1967) has shown that axial Bianchi V universes are reduced to Friedman universes with negative curvature. In our more detailed companion paper Valent, Tilquin & Schücker (2023) the interested reader may find an alternative proof (Valent, 2009).

Farnsworth’s result explains our interest in axial Bianchi IX universes on the theoretical side. On the observational side we note that a spherical Friedman universe is still compatible with data (Uzan, Kirchner & Ellis 2003), (Di Valentino, Melchiorri & Silk 2019), (Liu, Hu, Tang & Wu 2023) and we think it is worthwhile to consider a model featuring both small positive curvature and small anisotropies.

In section 2 we compute the Lemaître-Hubble diagram and Einstein’s equations in axial Bianchi IX universes. Our approach is pedestrian. The considered universe has four Killing vectors and therefore four conserved Noether quantities. With those we compute the geodesics of a photon coming from a supernova of ‘known’ absolute luminosity. Varying infinitesimally the emission time, we derive the direction-dependent redshift and varying infinitesimally the initial direction of the photon we derive the apparent luminosity.

In section 3 we linearize our results in small anisotropies $(c - a)/a$.

In section 4 we recall the exact solutions of Friedman’s equations in presence of a positive cosmological constant and comoving dust as given by Edwards (1972) in terms of Jacobi elliptic functions. They will be useful to speed up the fitting of the observed Lemaître-Hubble diagram to the one calculated in axial Bianchi IX universes with small anisotropies. Section 5 outlines our blueprint of the fitting procedure.

2 Axial Bianchi IX

Bianchi IX universes have compact, simply connected, homogeneous 3-spaces. The isometry group, $SO(3)$, is nonAbelian and compact, on the diametrical opposite of the Abelian isometry group of Bianchi I. Much is known about the dynamics of Bianchi IX universes.

Wald (1983): *The far future* of all initially expanding Bianchi I - VIII universes satisfying Einstein's equations with positive cosmological constant approaches the de Sitter universe exponentially fast. This only remains true for Bianchi IX universes if the cosmological constant is sufficiently large with respect to spacial curvature. "A positive cosmological constant provides an effective means of isotropizing homogeneous universes."

In *the far past*, Bianchi IX universes have complicated dynamics, oscillatory singularities, and chaos, (Misner 1969) (Belinsky, Khalatnikov & Lifshitz 1971 and 1972). Intriguingly the axial Bianchi IX universes are better behaved than the tri-axial ones. Dechant, Lasenby & Hobson (2009) and (2010) add a scalar field to axial Bianchi IX universes in order to soften the initial singularity. Let us stress that we will modestly remain in *our recent past*, $z < 6$.

Giani, Piattella & Kamenshchik (2022) have used Bianchi IX universes to model the gravitational collapse of matter inhomogeneities. They map the Bianchi IX field equations into those for a spherical Friedman universe filled with two scalar fields, only one scalar field in the axial case. We will meet the Klein-Gordon equation of this scalar field when we linearize the anisotropy, equation (52).

2.1 Metric

The axial Bianchi IX universe can be defined (Bianchi 1898; Terzis 2013) by:

$$d\tau^2 = dt^2 - \frac{1}{4}a^2 dx^2 - \frac{1}{4}(a^2 \cos^2 x + c^2 \sin^2 x) dy^2 - \frac{1}{4}c^2 dz^2 - \frac{1}{2}c^2 \sin x dy dz, \quad (2)$$

with the Euler angles $x \in (\frac{3}{2}\pi, \frac{3}{2}\pi + 2\pi)$, $y \in (0, 2\pi)$ and $z \in (0, 2\pi)$. It has four Killing vectors:

$$\sin y \partial_x - \tan x \cos y \partial_y + \frac{\cos y}{\cos x} \partial_z, \quad \cos y \partial_x + \tan x \sin y - \frac{\sin y}{\cos x} \partial_z, \quad \partial_y; \quad \partial_z. \quad (3)$$

(For vanishing anisotropies, $c - a = 0$, we recover the spherical Robertson-Walker universe.)

The Euler angles x, y, z are related to the familiar polar coordinates (King 1991) by:

$$\chi = \arccos \left(\cos \frac{x - \frac{3}{2}\pi}{2} \sin \frac{y - z}{2} \right), \quad x = 2 \arccos \sqrt{1 - \sin^2 \chi \sin^2 \theta} + \frac{3}{2}\pi, \quad (4)$$

$$\theta = \arctan \left(\tan \frac{x - \frac{3}{2}\pi}{2} / \cos \frac{y - z}{2} \right), \quad y = \varphi + \arccos \frac{\sin \chi \cos \theta}{\sqrt{1 - \sin^2 \chi \sin^2 \theta}}, \quad (5)$$

$$\varphi = \frac{y + z}{2}, \quad z = \varphi - \arccos \frac{\sin \chi \cos \theta}{\sqrt{1 - \sin^2 \chi \sin^2 \theta}}. \quad (6)$$

2.2 Geodesics

Now we are ready to prove that our coordinates are comoving with respect to test masses. With the four Killing vectors, Emmy Noether's theorem yields four conserved quantities on any geodesic $x^\mu(q)$ with affine parameter q and $\dot{} := d/dq$:

$$A := a^2 \sin y \dot{x} + (c^2 - a^2) \sin x \cos x \cos y \dot{y} + c^2 \cos x \cos y \dot{z}, \quad (7)$$

$$\bar{A} := a^2 \cos y \dot{x} - (c^2 - a^2) \sin x \cos x \sin y \dot{y} - c^2 \cos x \sin y \dot{z}, \quad (8)$$

$$B := (a^2 \cos^2 x + c^2 \sin^2 x) \dot{y} + c^2 \sin x \dot{z}, \quad (9)$$

$$C := c^2 \sin x \dot{y} + c^2 \dot{z}, \quad (10)$$

or equivalently

$$\dot{x} = \pm \frac{1}{a^2} \left[A^2 + \bar{A}^2 - \left(\frac{B \sin x - C}{\cos x} \right)^2 \right]^{1/2}, \quad \dot{y} = \frac{B - C \sin x}{a^2 \cos^2 x}, \quad (11)$$

$$\dot{z} = \frac{C}{c^2} - \sin x \frac{B - C \sin x}{a^2 \cos^2 x}, \quad A \cos y - \bar{A} \sin y = - \frac{B \sin x - C}{\cos x}. \quad (12)$$

Any dust test-particle with vanishing initial 3-velocity, $A = B = C = 0$, will remain at rest with respect to the coordinates (x, y, z) .

For a massless test particle, we have $\dot{x}^\mu g_{\mu\nu} \dot{x}^\nu = 0$ or equivalently:

$$\dot{t}^2 = \frac{A^2 + \bar{A}^2 + B^2 - C^2}{4a^2} + \frac{C^2}{4c^2}. \quad (13)$$

2.3 Redshift

We are now ready to compute the redshift in axial Bianchi IX universes. Since every Bianchi space is homogeneous (in the sense that it forms a single orbit under the group action), we may place the emitter at the north pole, $\chi_e = 0$. This choice considerably simplifies the computations, but we must pay due attention to the coordinate singularity at the poles. Equations (6) fix $x_e = \frac{3}{2}\pi$ and $z_e = y_e \pm \pi$.

At cosmic time t_e our emitter at the north pole radiates a photon. To have a unique solution of the geodesic equation in the interval $[q_e, q_0]$ we choose initial conditions at q_e :

$$\begin{aligned} t(q_e) &= t_e, & x(q_e) &= x_e = \frac{3}{2}\pi, & y(q_e) &= y_e, & z(q_e) &= z_e = y_e + \pi, \\ \dot{t}(q_e) &= \dot{t}_e > 0, & \dot{x}(q_e) &= R > 0, & \dot{y}(q_e) &= S, & \dot{z}(q_e) &= \dot{z}_e. \end{aligned} \quad (14)$$

They determine the conserved quantities by equations (7)-(10):

$$\frac{A}{\sin y_e} = \frac{\bar{A}}{\cos y_e} = a_e^2 R, \quad A^2 + \bar{A}^2 = a_e^4 R^2, \quad B = -C = c_e^2 (S - \dot{z}_e), \quad (15)$$

and evaluating the first of equations (12) at emission we obtain the initial condition

$$\dot{z}_e = \left[1 - 2 \frac{a_e^2}{c_e^2} \right] S, \quad (16)$$

where we have used the short-hand $a_e := a(t_e)$, $c_e := c(t_e)$. Other abbreviations will be useful:

$$s := \frac{2S}{R}, \quad W(t) := 2 \left[\frac{1}{a^2} + \frac{s^2}{c^2} \right]^{-1/2}, \quad f(x) := \frac{1 + \sin x}{\cos x}, \quad V(x) := [1 - s^2 f(x)^2]^{-1/2}. \quad (17)$$

In appendix A.1 we show how to eliminate the Noether constants from the geodesic equations (11,12,13) in favor of the initial conditions. Let us trade the equation for \dot{z} in favor of the equation for $\dot{\varphi} = (\dot{y} + \dot{z})/2$ and eliminate the affine parameter q in favor of cosmic time t . Then we remain with only three equations for the trajectory of the photon.

$$\frac{dx}{dt} = \frac{1}{a^2} \frac{W}{V}, \quad \frac{d\varphi}{dt} = \frac{1}{2} s \left[\frac{1}{a^2} - \frac{1}{c^2} \right] W, \quad \sin(y - y_e) = s f(x). \quad (18)$$

We suppose that the photon arrives today, $t_0 = t(q_0)$, in our telescope situated at $\vec{x}_0 := \vec{x}(q_0)$ and integrate the first two of these three equations by separation of variables,

$$\int_{t_e}^{t_0} \frac{W}{a^2} = \int_{x_e}^{x_0} V = \frac{2}{\sqrt{1 + s^2}} \arctan(\sqrt{1 + s^2} f_0 V_0), \quad (19)$$

$$\frac{s}{2} \int_{t_e}^{t_0} \left[\frac{1}{a^2} - \frac{1}{c^2} \right] W = \varphi_0 - \varphi_e = \varphi_0 - y_e - \frac{1}{2}\pi. \quad (20)$$

Consider now a second photon emitted at the north pole an atomic period T later in cosmic time than the first photon and arriving in our comoving telescope still at \vec{x}_0 at cosmic time $t_0 + T_D$. (\cdot_D stands for Doppler.) We suppose that the atomic periods, T and T_D , are much smaller than the time of flight $t_0 - t_e$ and the geodesics of the two photons, $x^\mu(q)$ and $\tilde{x}^\mu(q)$, $q \in [q_e, q_0]$ are infinitesimally close. For the second geodesic, the initial conditions at q_e are:

$$\begin{aligned} \tilde{t}(q_e) &= t_e + T, & \tilde{x}(q_e) &= x_e = \frac{3}{2}\pi, & \tilde{y}(q_e) &= \tilde{y}_e, & \tilde{z}(q_e) &= \tilde{y}_e + \pi, \\ \dot{\tilde{t}}(q_e) &> 0, & \dot{\tilde{x}}(q_e) &= \tilde{R} > 0, & \dot{\tilde{y}}(q_e) &= \tilde{S}, & \dot{\tilde{z}}(q_e) &= \left[1 - 2 \frac{\tilde{a}_e^2}{\tilde{c}_e^2} \right] \tilde{S}. \end{aligned} \quad (21)$$

We want to adjust the initial ‘velocity’ (or direction) of the second photon,

$$\tilde{y}_e =: y_e[1 + \delta], \quad \tilde{s} := \frac{2\tilde{S}}{\tilde{R}} =: s[1 + \epsilon], \quad (22)$$

such that its final comoving position coincides with that of the first photon, $\tilde{\vec{x}}_0 = \vec{x}_0$. The adjustment being infinitesimal, we may keep only linear terms in T , T_D , δ and ϵ . In this approximation, that we also indicate by \sim , we obtain

$$4 \left(\frac{T_D}{W_0} - \frac{T}{W_e} \right) \sim 0. \quad (23)$$

You find the details in appendix A.2. For non-vanishing T , we have the redshift

$$\underline{z} := \frac{T_D - T}{T} \sim \frac{W_0}{W_e} - 1. \quad (24)$$

This formula agrees with the general definition of redshift, that you find in Pierre Fleury’s beautiful thesis (Fleury 2015) as equation (1.71).

To avoid confusion with the third Euler angle, we underline the redshift \underline{z} temporarily.

2.4 Apparent luminosity

The trajectory of our photon is described by the lightlike geodesic $\vec{x}(t)$ with initial conditions (14) and given by equations (18-20). We obtained the redshift from the infinitesimal variation of the initial conditions in (14):

$$t_e \rightarrow t_e + T, \quad y_e \rightarrow y_e(1 + \delta), \quad s \rightarrow s(1 + \epsilon). \quad (25)$$

Requiring that the two geodesics end at the same point in space $\vec{x}_0 = \tilde{\vec{x}}_0$ we computed the proper time difference at reception $T_D = \tilde{t}_0 - t_0$. For the apparent luminosity we need two more infinitesimally close lightlike geodesics

$$\vec{x}_\delta(t) = \vec{x}(t) + \vec{\delta}(t) \quad \text{and} \quad \vec{x}_\epsilon(t) = \vec{x}(t) + \vec{\epsilon}(t) \quad (26)$$

with varied spatial initial conditions $y_e \rightarrow y_e(1 + \delta)$ and $s \rightarrow s(1 + \epsilon)$ respectively. All three geodesics are emitted simultaneously at t_e from the point \vec{x}_e . The two 3-vectors $\vec{\delta}(t)$ and $\vec{\epsilon}(t)$, which should not be confused with the infinitesimal numbers δ and ϵ , are interpreted as tangent vectors at $\vec{x}(t)$ just as the velocity $\vec{x}'(t)$. The prime denotes the derivative with respect to cosmic time t . As a function of time, $\vec{\delta}(t)$ and $\vec{\epsilon}(t)$ define a family of infinitesimal triangles. They are perpendicular to the trajectory $\vec{x}(t)$. The triangles represent the beam of photons emitted by the supernova at $\vec{x}(t_e)$. The photons illuminate a triangular photo-plate now and here $\vec{x}(t_0)$, see figure 1. The plate is placed perpendicular to the beam and its area is $dS(t_0) =: dS_0$. Our task is to compute the area $dS(t)$ of the infinitesimal triangles and their solid angle $d\Omega_e$ at emission. Then the apparent luminosity is:

$$\ell = L \frac{d\Omega_e}{dS_0} (z + 1)^{-2}, \quad (27)$$

with the absolute luminosity L of the supernova.

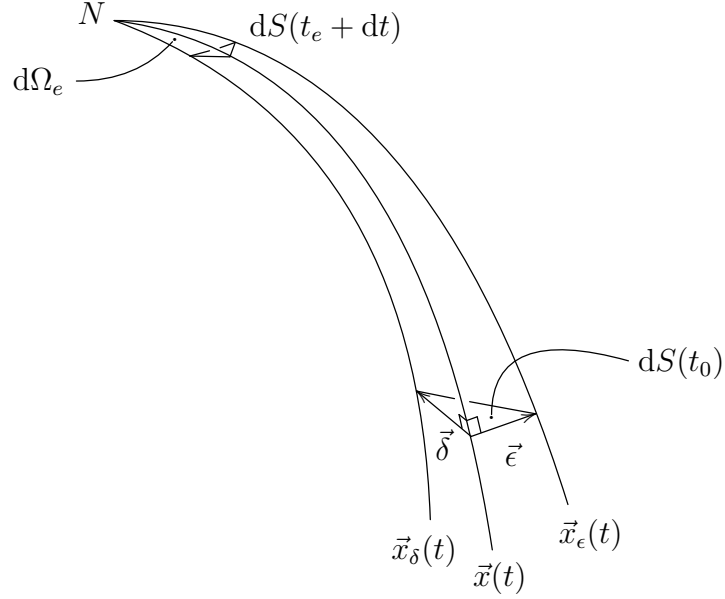


Figure 1: Three infinitesimally close geodesics and two perpendicular triangles

As detailed in appendix B, the infinitesimal triangles defined by $\vec{\delta}(t)$ and $\vec{\epsilon}(t)$ are perpendicular to the ray $\vec{x}'(t)$ and their areas as a function of time $dS(t)$, see figure 1, are given by

$$\begin{aligned} dS &= \frac{1}{2} \left((\vec{\delta} \cdot \vec{\delta})(\vec{\epsilon} \cdot \vec{\epsilon}) - (\vec{\delta} \cdot \vec{\epsilon})^2 \right)^{1/2} \\ &= \frac{1}{2} \delta \epsilon y_e \frac{s}{1+s^2} \frac{a^2 c}{W} (1 + \sin x) \left| 1 - \frac{1}{2} \frac{I_3}{fV} \right|, \end{aligned} \quad (28)$$

where we denote by $\vec{\delta} \cdot \vec{\epsilon}$ the negative of the scalar product of 3-vectors defined by the spatial part of the metric tensor $g_{\mu\nu}$ in equation (2), and with

$$I_3(t) := \frac{1}{4} \int_{t_e}^t \frac{W^3}{a^2} \left[\frac{1}{a^2} - \frac{1}{c^2} \right]. \quad (29)$$

Of course at emission time t_e the area vanishes and to compute the solid angle it sustains at the north pole $\vec{x}(t_e)$ we evaluate $dS(t_e + dt)$ to leading order in dt . From the first of equations (18) we have $dx \sim W_e/a_e^2 dt$ and:

$$1 + \sin x(t_e + dt) \sim \frac{1}{2} \frac{W_e^2}{a_e^4} dt^2, \quad f(x(t_e + dt)) \sim \frac{1}{2} \frac{W_e}{a_e^2} dt. \quad (30)$$

We linearize the integral I_3 defined in equation (29) with respect to dt ,

$$I_3(t_e + dt) \sim \frac{1}{4} \frac{W_e^3}{a_e^2} \left[\frac{1}{a_e^2} - \frac{1}{c_e^2} \right] dt. \quad (31)$$

Therefore

$$1 - \frac{1}{2} \frac{I_3}{fV} = \frac{1}{4} \frac{1+s^2}{c_e^2} W_e^2 + O(dt) \quad \text{and} \quad dS(t_e + dt) \sim \frac{1}{16} \delta\epsilon y_e s \frac{W_e^3}{a_e^2 c_e} dt^2. \quad (32)$$

Finally the solid angle is

$$d\Omega_e = \frac{dS(t_e + dt)}{4\pi dt^2} = \frac{\delta\epsilon}{64\pi} y_e s \frac{W_e^3}{a_e^2 c_e}, \quad (33)$$

and the apparent luminosity:

$$\ell = \frac{L}{32\pi} \frac{W_e^5 (1+s^2)}{a_e^2 c_e a_0^2 c_0 W_0 (1+\sin x_0)} \left| 1 - \frac{1}{2} \frac{I_{30}}{f_0 V_0} \right|^{-1}. \quad (34)$$

Note that the initial condition y_e drops out from the redshift and the apparent luminosity. Therefore only the initial condition s remains to be interpreted. It is related to the angle between the direction here and now $-\vec{x}'(t_0)$ pointing to the supernova at the north pole and the privileged direction of the axial Bianchi IX universe, the fourth Killing vector ∂_z . Let us denote this angle by γ_0 . We have:

$$\cos \gamma = \frac{-\vec{x}' \cdot \vec{\partial}_z}{\sqrt{\vec{\partial}_z \cdot \vec{\partial}_z}} = \frac{s}{\sqrt{\frac{c^2}{a^2} + s^2}} \quad \text{or} \quad s = \frac{c}{a} \cot \gamma = \frac{c_0}{a_0} \cot \gamma_0. \quad (35)$$

2.5 Einstein's equations

To write down the non-vanishing components of the Einstein tensor we will use the notations $H := a'/a$ and $H_c := c'/c$,

$$G_{tt} = 3H^2 + 2H(H_c - H) + \frac{1}{a^2} \left(4 - \frac{c^2}{a^2} \right), \quad (36)$$

$$G_{xx} = -\frac{a^2}{4} \left[H' + H_c' + H^2 + H_c^2 + HH_c + \frac{c^2}{a^4} \right], \quad (37)$$

$$G_{zz} = -\frac{c^2}{4} \left[2H' + 3H^2 + \frac{1}{a^2} \left(4 - 3\frac{c^2}{a^2} \right) \right], \quad (38)$$

$$G_{yy} = \cos^2 x G_{xx} + \sin^2 x G_{zz}, \quad G_{yz} = \sin x G_{zz}. \quad (39)$$

Therefore we may assume that the energy-momentum tensor has only one non-vanishing component, the mass density $T_{tt} = \rho(t)$, ‘matter is comoving dust’. The covariant conservation of energy, $\rho' + (2H + H_c)\rho = 0$, yields mass conservation:

$$\rho(t) = a_0^2 c_0 \frac{\rho_0}{a(t)^2 c(t)}, \quad a_0 := a(t_0), \quad c_0 := c(t_0), \quad \rho_0 := \rho(t_0). \quad (40)$$

The Einstein equations read:

$$3H^2 + 2H(H_c - H) + \frac{1}{a^2} \left(4 - \frac{c^2}{a^2} \right) = \Lambda + 8\pi G \rho, \quad (41)$$

$$H' + H'_c + H^2 + H_c^2 + HH_c + \frac{c^2}{a^4} = \Lambda, \quad (42)$$

$$2H' + 3H^2 + \frac{1}{a^2} \left(4 - 3 \frac{c^2}{a^2} \right) = \Lambda. \quad (43)$$

Let us use the mass conservation to reduce the three Einstein equations to the tt component and to the xx component minus the zz component. We obtain the equivalent system:

$$3H^2 + 2H(H_c - H) + \frac{1}{a^2} \left(4 - \frac{c^2}{a^2} \right) = \Lambda + 8\pi G \rho_0 \frac{a_0^2 c_0}{a^2 c}, \quad (44)$$

$$(H_c - H)' + (2H + H_c)(H_c - H) - \frac{4}{a^2} \left(1 - \frac{c^2}{a^2} \right) = 0. \quad (45)$$

3 Linearizing axial Bianchi IX

3.1 Linearizing Einstein's equations

Consider the Robertson-Walker universe with one scale factor as function of cosmic time $a_F(t)$, \cdot_F for Friedman, and its Hubble parameter $H_F := a'_F/a_F$. The first Friedman equation is the tt component of the Einstein equation and can be written

$$3H_F^2 + 3 \frac{\kappa}{a_F^2} = \Lambda + 8\pi G \rho_{F0} \frac{a_{F0}^3}{a_F^3}, \quad (46)$$

with four parameters:

- the ‘initial’ condition today $a_F(t_0) := a_{F0}$,
(Of course we mean ‘final’, because we want to compute the past.)
- the cosmological constant Λ ,
- $8\pi G \rho_{F0}$ with G being Newton's constant and ρ_{F0} the mass density of dust today,
- $\kappa = 0, 1, -1$ for the 3-spaces with zero, positive and negative curvature.

A fifth parameter is important: today's Hubble parameter also more appropriately called Lemaître-Hubble constant, $H_F(t_0) =: H_{F0}$. Its absolute value is determined by the first Friedman equation evaluated today. At the same time the choice of the other four parameters must obey the inequality,

$$\Lambda + 8\pi G \rho_{F0} - 3 \frac{\kappa}{a_{F0}^2} \geq 0. \quad (47)$$

Note also that in the flat case $\kappa = 0$, the initial condition a_{F0} is not essential.

Being a first order ordinary differential equation, the Friedman equation has a unique local solution once we have chosen the four parameters in compliance with the inequality.

If the universe is not static, the first Friedman equation (46) implies the second Friedman equation (the xx component of the Einstein equation),

$$2 H'_F + 3 H_F^2 + \frac{\kappa}{a_F^2} = \Lambda, \quad (48)$$

and the mass conservation, $\rho'_F + 3 H_F \rho_F = 0$, is satisfied if we set

$$\rho_F := \rho_{F0} \frac{a_{F0}^3}{a_F^3}. \quad (49)$$

For a static universe (Einstein) we must have $\kappa = 1$ and $a_{F0}^{-2} = \Lambda = 4\pi G \rho_{F0}$. It has seven Killing vectors, but it is unstable. From now on we will ignore the static universe and use the standard dimensionless parameters:

$$\Omega_{m0} := \frac{8\pi G \rho_{F0}}{3H_{F0}^2}, \quad \Omega_{\Lambda0} := \frac{\Lambda}{3H_{F0}^2}, \quad \Omega_{\kappa0} := \frac{-\kappa}{a_{F0}^2 H_{F0}^2} = 1 - \Omega_{m0} - \Omega_{\Lambda0}. \quad (50)$$

Then a big bang or a bounce occurs and we take it as origin of cosmic time $a_F(0) = 0$ or $H_F(0) = 0$.

Now consider positive curvature, $\kappa = 1$. The following linearization in $\eta(t)$ is mandatory:

$$a = a_F [1 - \frac{1}{2}\eta], \quad c = a_F [1 + \eta]. \quad (51)$$

Indeed in Bianchi I universes, $\kappa = 0$, we used the simpler linearization with $a = a_F$, implying however $\rho_0 \neq \rho_{F0}$ (Schücker et al. 2014). For Bianchi V and IX this simpler linearization together with Einstein's equations implies isotropy, $\eta = 0$. In our long version (Valent et al. 2022) we justify our linearization (51) and show that it implies $\rho_0 = \rho_{F0}$.

Let us linearize now the two Einstein equations in Bianchi IX universes under the form (44) and (45) using (51). To first order in η we obtain the first Friedman equation (46) and the Klein-Gordon equation for η .

$$\eta'' + 3 H_F \eta' + 8 \frac{\eta}{a_F^2} \sim 0. \quad (52)$$

Note that the function η is the Klein-Gordon field in Giani, Piattella & Kamenshchik (2022) and our equation (52) agrees with their equation (3.6).

Our four essential initial conditions, a_0, c_0, H_0, H_{c0} , fix ρ_0 by the tt component of the Einstein equation (44). They translate into the four essential initial conditions:

$$a_{F0} = \frac{2}{3}a_0 + \frac{1}{3}c_0, \quad H_{F0} \sim \frac{2}{3}H_0 + \frac{1}{3}H_{c0}, \quad \eta_0 = \frac{c_0 - a_0}{a_0 + \frac{1}{2}c_0}, \quad \eta'_0 \sim \frac{3}{2}(H_{c0} - H_0). \quad (53)$$

We call the last two ‘ellipticity’ and ‘Hubble stretch’.

3.2 Linearizing redshift and apparent luminosity

We start by linearizing $W(t)$ defined by the second of equations (17),

$$W \sim \frac{2}{\sqrt{1+s^2}} a_F \left[1 - \frac{1}{2} \frac{1-2s^2}{1+s^2} \eta \right], \quad (54)$$

from which we obtain the linearized redshift,

$$\underline{z} + 1 \sim \frac{a_{F0}}{a_{Fe}} \left[1 - \frac{1}{2} \frac{1-2s^2}{1+s^2} (\eta_0 - \eta_e) \right]. \quad (55)$$

Next we linearize the integral $I_3(t)$, equation (29),

$$I_3 \sim \frac{6}{(1+s^2)^{3/2}} \int_{t_e}^t \frac{\eta}{a_F}, \quad (56)$$

and linearize the apparent luminosity:

$$\ell \sim \frac{L}{2\pi} \frac{a_{Fe}^2}{a_{F0}^4} \frac{1}{(1+s^2)(1+\sin x_0)} \left[1 + \frac{1}{2} \frac{1-2s^2}{1+s^2} (\eta_0 - 5\eta_e) + \frac{3}{(1+s^2)^{3/2}} \frac{\chi_{e0} \bar{\eta}_{e0}}{f_0 V_0} \right], \quad (57)$$

with the definitions:

$$\chi_e(t) := \int_{t_e}^t \frac{1}{a_F}, \quad \chi_{e0} := \chi_e(t_0), \quad \bar{\eta}_e(t) := \frac{1}{\chi_e(t)} \int_{t_e}^t \frac{\eta}{a_F}, \quad \bar{\eta}_{e0} := \bar{\eta}_e(t_0). \quad (58)$$

Remember that we used χ for the radial coordinate in equation (6). This χ is the geodesic distance from the north pole on the 3-sphere. We have set the speed of light to unit. Therefore the conformal time $\chi_e(t)$ coincides with the comoving geodesic distance of our photon emitted at the north pole $\chi = 0$ at cosmic time t_e in the underlying Friedman universe, $\eta = 0$.

To compute the apparent luminosity of our photon in the axial Bianchi IX universe in linear approximation, we still need $f(x)V(x)$ to zeroth order in $x - x_F$ and $1 + \sin x$ to first order. To this end we linearize equation (19) and obtain:

$$f(x_F)V(x_F) = \frac{\tan \chi_e}{\sqrt{1+s^2}} \quad \text{and} \quad 1 + \sin x \sim \frac{2}{1+s^2} \sin^2 \chi_e \left[1 + \frac{1+4s^2}{1+s^2} \frac{\chi_e \bar{\eta}_e}{\tan \chi_e} \right]. \quad (59)$$

Now, the apparent luminosity takes the form:

$$\ell \sim \ell_F \left[1 + \frac{1}{2} \frac{1-2s^2}{1+s^2} \left(\eta_0 - 5\eta_e + 4 \frac{\chi_{e0}}{\tan \chi_{e0}} \bar{\eta}_{e0} \right) \right] \quad (60)$$

with

$$\ell_F = \frac{L}{4\pi a_{F0}^2 \sin^2 \chi_{e0}} \left(\frac{a_{Fe}}{a_{F0}} \right)^2. \quad (61)$$

Note that the initial condition s appears in the linearized redshift \underline{z} (dropping the underline) and in the linearized apparent luminosity always multiplied by η . Therefore to first order,

we may replace s here simply by $s \sim \cot \gamma_0$. Note that in this approximation the angle γ also coincides with the coordinate θ , which is constant for geodesics coming from the north pole. Therefore:

$$z + 1 \sim \frac{a_{F0}}{a_{Fe}} \left[1 - \frac{1 - 3 \cos^2 \theta}{2} (\eta_0 - \eta_e) \right], \quad (62)$$

$$\ell \sim \ell_F \left[1 + \frac{1 - 3 \cos^2 \theta}{2} \left(\eta_0 - 5\eta_e + 4 \frac{\chi_{e0}}{\tan \chi_{e0}} \bar{\eta}_{e0} \right) \right]. \quad (63)$$

In the limit of zero curvature, a_0 and $c_0 \rightarrow \infty$, we have

$$\lim \sin \chi_{e0} = \chi_{e0}, \quad \lim \frac{\chi_{e0}}{\tan \chi_{e0}} = 1, \quad (64)$$

and the differential equation for η in Bianchi IX (52) reduces to the one in Bianchi I. Taking due account of our change of definitions, $\eta_I = \frac{3}{2}\eta_{IX}$ and $\chi_I = \int 1/a$ while here $\chi_{IX} = \int 1/a_F$, we reproduce our perturbative results (Schücker et al. 2014) of axial Bianchi I.

Note the $\cos^2 \theta$ in equations (62) and (63) ensuring that the Lemaître-Hubble diagram in Bianchi I and IX universes has forward-backward symmetric anisotropies (quadrupole). They can be distinguished easily from the anisotropies induced by a peculiar velocity of the observer (the kinetic dipole), that do not share this symmetry.

4 Exact solutions of Friedman's equations with comoving dust

To speed up the fitting of axial Bianchi IX universes with the Lemaître-Hubble diagram, it will be useful to have exact solutions of the Friedman equations (46).

Exact solutions of the Friedman equations in presence of a cosmological constant, curvature, dust and radiation are well-known, for example in terms of Weierstraß elliptic functions (Lemaître 1933; Coquereaux & Grossmann 1982; Coquereaux 2015). We will not have to include radiation, which considerably simplifies the solutions and we will use Jacobi elliptic functions, following Edwards (1972).

4.1 The scale factor a_F as function of conformal time χ

Let us change the independent variable in the scale factor a_F from cosmic time t to the dimensionless conformal time = comoving geodesic distance,

$$\chi(t) := \int_0^t \frac{1}{a_F}, \quad 0 \leq t. \quad (65)$$

We will set the big bang at $t = 0$, $a_F(0) = 0$, but the corresponding singularity will be integrable. Note the link with our former definition (58):

$$\chi_e(t) = \chi(t) - \chi(t_e). \quad (66)$$

By abuse of notations we write the inverse function of $\chi(t)$ as $t(\chi)$.

Let us also change dimensionless parameters assuming that the cosmological constant is positive:

$$\Lambda > 0, \quad \gamma := 4 \frac{\Omega_{m0}}{\Omega_{\Lambda 0}}, \quad \nu := -\frac{4}{3} \frac{\Omega_{\kappa 0}}{\Omega_{\Lambda 0}}. \quad (67)$$

Note that ν and κ carry the same signs or vanish both. Let us assume that

$$\gamma^2 - \nu^3 = 16 \frac{\Omega_{m0}^2}{\Omega_{\Lambda 0}^2} \left(1 + \frac{4}{27} \frac{\Omega_{\kappa 0}^3}{\Omega_{\Lambda 0} \Omega_{m0}^2} \right) > 0, \quad (68)$$

is positive. This implies that there is a big bang. If $\gamma^2 - \nu^3$ vanishes we have Einstein's static universe with seven Killing vectors. Universes with negative $\gamma^2 - \nu^3$ are spherical and undergo one bounce. They contain the maximally symmetric de Sitter spacetimes (positive curvature, ten Killing vectors). Nevertheless we will ignore this last class, because it is frankly incompatible with today's observations, which we would like to try and fit in section 5 with universes breaking minimally the isometry group in the spaces of simultaneity (positive curvature, four Killing vectors).

Since $\gamma^2 - \nu^3$ is positive, a further parameter,

$$\tilde{s} := -\frac{1}{2} \left(\gamma + \sqrt{\gamma^2 - \nu^3} \right)^{1/3} - \frac{1}{2} \left(\gamma - \sqrt{\gamma^2 - \nu^3} \right)^{1/3}, \quad (69)$$

is real and $\tilde{s}^2 - \nu > 0$. This inequality allows us to define three positive constants

$$A := \sqrt{\tilde{s}^2 - \frac{3}{4}\nu} < B := \sqrt{3\tilde{s}^2 - \frac{3}{4}\nu}, \quad k^2 := \frac{1}{2} + \frac{3}{4} \frac{\tilde{s}^2 - \nu/2}{AB}, \quad (70)$$

and to check that $k^2 < 1$ since we have

$$k^2(1 - k^2) = \frac{4A^2B^2 - 9(\tilde{s}^2 - \nu/2)^2}{16A^2B^2} = 3 \frac{\tilde{s}^2(\tilde{s}^2 - \nu)}{16A^2B^2} > 0. \quad (71)$$

(Of course the constants A and B have nothing to do with the conserved quantities defined in equations (7) and (9).)

We need one last dimensionless positive constant,

$$\sigma := a_{F0} \sqrt{\frac{\Lambda AB}{3}}. \quad (72)$$

Now the solution of Friedman's equation (46) can be written explicitly as function of conformal time using the Jacobi and related functions defined in appendix C (suppressing the argument k^2),

$$a_F(t(\chi)) = a_{F0} |\tilde{s}| \frac{A}{A+B} \frac{1 - \text{cn}(\sigma\chi)}{\text{cn}(\sigma\chi) - \text{cn}(\sigma\hat{\chi})}, \quad \text{cn}(\sigma\hat{\chi}) := \frac{A-B}{A+B}. \quad (73)$$

The big bang takes place at $\chi = 0$, $t(0) = 0$, because $\text{cn } 0 = 1$. The age of the universe in conformal time is:

$$\chi_0 = \frac{1}{\sigma} \arccn \frac{A(1 + |\tilde{s}|) - B}{A(1 + |\tilde{s}|) + B}. \quad (74)$$

Note that at finite conformal time $\hat{\chi}$ the scale factor tends to infinity. The corresponding cosmic time $t(\hat{\chi})$ is infinite, indeed the integral

$$\int_0^\infty \frac{dt}{a_F(t)} = \hat{\chi} \quad (75)$$

is convergent.

The relation (73) was first given by Edwards (1972).

4.2 Cosmic time t as function of conformal time χ

We use the first of the four Theta functions $\theta_1(v, q)$ defined in appendix C and Jacobi's notations:

$$q := e^{-\pi K'/K}, \quad H(u) := \theta_1\left(\frac{\pi u}{2K}, q\right), \quad \zeta(u) := \frac{d}{du} \ln H(u). \quad (76)$$

(The function $H(u)$ has nothing to do with the Hubble parameter.) Then we can write the cosmic time as function of conformal time

$$t(\chi) = \sqrt{\frac{3}{\Lambda}} \left\{ \frac{1}{2} \ln \left(\frac{H(\sigma(\chi + \hat{\chi}))}{H(\sigma(-\chi + \hat{\chi}))} \frac{\hat{s} \operatorname{dn}(\sigma\chi) + \hat{d} \operatorname{sn}(\sigma\chi)}{\hat{s} \operatorname{dn}(\sigma\chi) - \hat{d} \operatorname{sn}(\sigma\chi)} \right) - \left(\zeta(\sigma\hat{\chi}) + \frac{\hat{d}}{\hat{s}} \right) \sigma\chi \right\}, \quad (77)$$

with the abbreviations:

$$\hat{s} := \operatorname{sn} \hat{u} = 2 \frac{\sqrt{AB}}{A+B}, \quad \hat{c} := \operatorname{cn} \hat{u} = \frac{A-B}{A+B}, \quad \hat{d} = \operatorname{dn} \hat{u} = \frac{|\tilde{s}|}{A+B}, \quad \hat{u} = \sigma\hat{\chi}. \quad (78)$$

An *ab initio* proof of the expressions $a_F(t(\chi))$ and $t(\chi)$ can be found in our long version (Valent et al. 2022).

Unfortunately we do not have the explicit inverse $\chi(t)$, which we compute numerically by interpolation.

5 The Lemaître-Hubble diagram in axial Bianchi IX universes with small anisotropies

The Lemaître-Hubble diagram is the parametric plot $(\ell(t_e), z(t_e))$ whose parameter is the cosmic emission time t_e . As the light arriving in our telescope cannot tell us its emission time it is convenient to use as parameter the conformal emission time $\chi(t_e)$ instead of the cosmic emission time t_e . Then the fit with the supernova data follows the following steps:

1. Choose a spherical or flat Friedman universe with comoving dust characterized by three positive parameters: H_{F0} , $\Omega_{\Lambda0}$, Ω_{m0} , such that

$$\Omega_{\Lambda0} + \Omega_{m0} \geq 1 \quad (\text{positive or zero curvature, } \Omega_{\kappa0} \leq 0), \quad (79)$$

$$1 + \frac{4}{27} \frac{\Omega_{\kappa0}^3}{\Omega_{\Lambda0}\Omega_{m0}^2} > 0 \quad (\text{initial big bang}). \quad (80)$$

Then the age of the universe in conformal time χ_0 is given by equation (74) and in cosmic time $t_0 = t(\chi_0)$ by equation (77). The scale factor today is

$$a_{F0} = \frac{1}{H_{F0}\sqrt{-\Omega_{\kappa0}}}. \quad (81)$$

For any conformal time χ the scale factor $a_\chi(\chi) := a_F(t(\chi))$ is given by equation (73).

2. Fix the z -axis in the sky by two parameters, e.g. (right ascension, declination).
3. Choose two more *small* parameters: the final conditions of the infinitesimal anisotropy $\eta(t)$ today. Since we will work with the conformal time, let us define $\eta_\chi(\chi) := \eta(t(\chi))$ and the final conditions today by:

$$\eta_\chi(\chi_0) = \eta(t_0) = \eta_0 \quad \text{'ellipticity'}, \quad (82)$$

$$\frac{d}{d\chi}\eta_\chi(\chi_0) = a_{F0} \frac{d}{dt}\eta(t_0) \quad \text{'Hubble stretch'}. \quad (83)$$

Both should be smaller in absolute value than 10 %. Note that in the flat case the ellipticity vanishes by the choice $a_0 = c_0$ and Bianchi I only has the Hubble stretch.

4. Rewriting equation (52) in terms of conformal time, we have:

$$\frac{d^2}{d\chi^2}\eta_\chi + 2H_\chi \frac{d}{d\chi}\eta_\chi + 8\kappa\eta_\chi \sim 0, \quad \kappa = 1, 0, \quad (84)$$

with the conformal Hubble parameter

$$H_\chi := \frac{d}{d\chi}a_\chi/a_\chi = \sigma(1 - \widehat{c}) \frac{\text{sn } u \text{ dn } u}{(1 - \text{cn } u)(\text{cn } u - \widehat{c})}. \quad (85)$$

Solve this linear differential equation numerically for times prior to χ_0 with the final conditions: ellipticity and Hubble stretch.

5. Choose a supernova with its redshift z , luminosity ℓ_{obs} and its direction. Let θ be the angle between this direction and the chosen z -axis.

Invert numerically

$$z + 1 \sim \frac{a_{F0}}{a_\chi(\chi_e)} \left[1 - \frac{1 - 3\cos^2\theta}{2} (\eta_0 - \eta_\chi(\chi_e)) \right] \quad (86)$$

to obtain the emission time $\chi_e := \chi(t_e)$ for a given redshift and angle θ . Attention, the conformal emission time is a number and should not be confused with the function $\chi_e(t) := \int_{t_e}^t a_F^{-1}$, equation (58). We have $\chi_e(t_0) =: \chi_{e0} = \chi_0 - \chi_e$ and $\eta_\chi(\chi_e) = \eta(t_e) = \eta_e$.

For consistency of the linearization, η_e must remain smaller in absolute value than 10 %.

6. Evaluate numerically the integral

$$\bar{\eta}_{e0} := \frac{1}{\chi_{e0}} \int_{\chi_e}^{\chi_0} \eta_\chi. \quad (87)$$

7. Compute the theoretical apparent luminosity,

$$\ell \sim \frac{L}{4\pi a_{F0}^2 \sin^2 \chi_{e0} (z+1)^2} \left[1 + \frac{1-3\cos^2\theta}{2} \left(\eta_0 - 5\eta_e + 4 \frac{\chi_{e0}}{\tan \chi_{e0}} \bar{\eta}_{e0} \right) \right], \quad (88)$$

and compare it to the observed apparent luminosity ℓ_{obs} .

8. Let Δ_i be $\ell_{obs} - \ell$ for the i th supernova and let V be the covariance matrix encoding the experimental error bars. Define $\chi^2 := \sum_{ij} \Delta_i V_{ij}^{-1} \Delta_j$. (Of course this χ^2 has nothing to do with conformal time.)

9. Minimize χ^2 over the set of the seven parameters:

H_{F0} , $\Omega_{\Lambda 0}$, Ω_{m0} , (right ascension, declination), ellipticity and Hubble stretch in their domains of definition.

Axial Bianchi I is the five-parameter sub-model with vanishing curvature, $\Omega_{\Lambda 0} + \Omega_{m0} = 1$, and vanishing ellipticity, $\eta_0 = 0$.

Note that the direction dependence is captured by the quadrupole coefficient $(1-3\cos^2\theta)/2$ in both redshift and apparent luminosity as function of emission time. This coefficient varies from -1 for $\theta = 0$ to 1/2 for $\theta = 90^\circ$ and vanishes around $\theta = 54.7^\circ$. In this direction the Lemaître-Hubble diagrams of the axial Bianchi IX and Bianchi I universes coincide with the direction-independent Lemaître-Hubble diagrams of their underlying spherical and flat Friedman universes.

As an example we display in figure 2 the Lemaître-Hubble diagrams $\ell(z)$ for $\theta = 0$ simultaneously for the Bianchi IX universe with $\Omega_{\Lambda 0} = 0.35$, $\Omega_{m0} = 0.75$, $\eta_0 = 0$, $d/d\chi \eta_\chi(\chi_0) = 0.04$ and the Bianchi I universe with $\Omega_{\Lambda 0} = 0.3$, $\Omega_{m0} = 0.7$, $\eta_0 = 0$, $d/d\chi \eta_\chi(\chi_0) = -0.01$ and their underlying Friedman universes.

The example suggests that small positive curvature and small anisotropies do co-exist peacefully in axial Bianchi IX universes during our recent past.

In 2014 we confronted the Bianchi I model with the 740 type 1a supernovae below a redshift of $z = 1.3$ in the Joint Light curve Analysis by Betoule et al. (2014) and found only a 1- σ signal (Schücker et al. 2014).

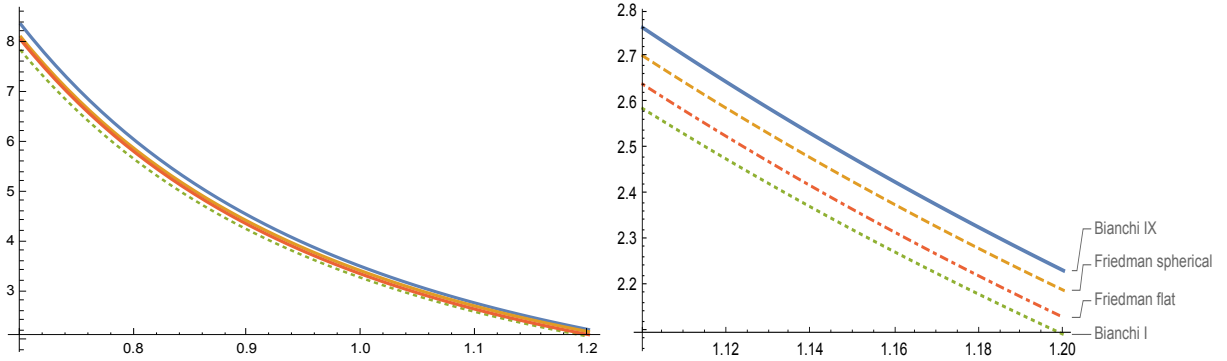


Figure 2: apparent luminosity ℓ in arbitrary units versus redshift z
blue, continuous: Bianchi IX, orange, dashed: Friedman spherical,
green, dotted: Bianchi I, red, dashed dotted: Friedman flat

Therefore we think that a fit of the seven-parameter axial Bianchi IX model to the Lemaître-Hubble diagram of supernovae becomes reasonable only once we can include the data expected from the Vera Rubin Observatory, the James Webb Space Telescope and the Chinese Space Station Telescope.

Also in 2014 Cea (2014) fitted the axial Bianchi I model to the WMAP and Planck data at redshift 1090. He also found a $1-\sigma$ signal. Although his Hubble stretch has opposite sign and is smaller than ours by eight orders of magnitude, our results are compatible with his.

Again in 2014 Darling (2014) used the tri-axial Bianchi I model (seven parameters) to fit the apparent motion of 429 extra-galactic radio sources measured by Titov & Lambert (2013) using Very Long Baseline Interferometry. His main Hubble stretch has the same sign as ours but is ten times larger and the results are again compatible statistically.

Waiting and preparing for the mentioned supernovae to be observed, a combined analysis of axial Bianchi IX universes with the Lemaître-Hubble diagram, the Cosmic Microwave Background, the drift of extra-galactic sources and Baryonic Acoustic Oscillations (and maybe with weak lensing or black-hole mergers) is called for.

6 Conclusions

Our motivation for this work is to use Bianchi universes to search for anisotropies in the Lemaître-Hubble diagram of type 1a supernovae. These universes are necessarily close to the maximally symmetric Friedman universes and, if we want to add only the minimal number of degrees of freedom to the fit of the standard model, the Bianchi universes must have four isometries, i.e. are axial. Therefore we remain only with axial Bianchi I, V and IX universes, see the cartoon in figure 3.

Axial Bianchi V universes are incompatible with comoving dust (Farnsworth 1967), an asymmetry between negative and positive curvature that we find most remarkable.

Therefore we computed the Lemaître-Hubble diagram for axial Bianchi IX universes. In the limit of zero curvature, it reproduces the diagram for axial Bianchi I universes.

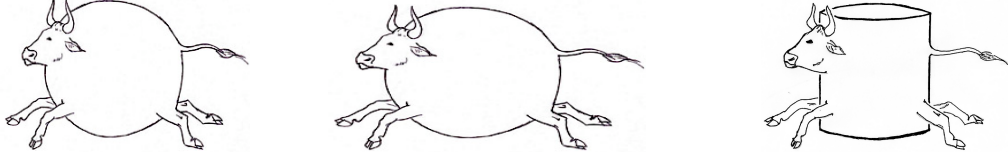


Figure 3: Robertson-Walker; axial Bianchi I, V, IX; Bianchi II, III, IV, VI_h, VIII

We completely agree with Aluri, Cea et al. (2023) and join their plea for tests of the cosmological principle in synergy of all available cosmological probes. Axial Bianchi IX universes are an excellent choice for such a test.

Acknowledgements: We thank our two referees for their constructive feedback.

The project leading to this publication has received funding from Excellence Initiative of Aix Marseille University - A*MIDEX, a French “Investissements d’Avenir” programme (AMX-19-IET-008 - IPhU).

Data availability: The data underlying this article will be shared on reasonable request to the corresponding author.

A Redshift

A.1 First photon

We have the following derivatives,

$$f_x(x) := \frac{d}{dx} f(x) = \frac{1 + \sin x}{\cos^2 x}, \quad \frac{d}{dx} f_x(x) = f(x) f_x(x), \dots; \quad (89)$$

relations,

$$f(x) = \tan \frac{x - \frac{3}{2}\pi}{2}, \quad f_x(x) = \frac{1}{1 - \sin x} = \frac{1 + f^2}{2}; \quad (90)$$

integrals,

$$\int V = \frac{2}{\sqrt{1 + s^2}} \arctan(\sqrt{1 + s^2} f V), \quad \int (1 + f^2) V^3 = 2 f V; \quad (91)$$

and limits at the north pole,

$$\lim_{x \rightarrow x_e} f(x) = 0, \quad \lim_{x \rightarrow x_e} f_x(x) = \frac{1}{2}, \dots. \quad (92)$$

Equations (13), (11)-(12) become

$$\dot{t} = a_e^2 R W^{-1}, \quad \dot{x} = \frac{a_e^2}{a^2} R V^{-1}, \quad (93)$$

$$\dot{y} = \frac{a_e^2}{a^2} R s f_x, \quad \dot{z} = -\dot{y} + a_e^2 R s \left[\frac{1}{a^2} - \frac{1}{c^2} \right], \quad (94)$$

$$\sin(y - y_e) = s f(x). \quad (95)$$

Let us compute the initial polar angles (6). For θ we use equation (95) and write

$$\tan \theta = \frac{f}{\cos \frac{y-z}{2}} = \frac{1}{s} \frac{\sin(y - y_e)}{\cos \frac{y-z}{2}} = \frac{1}{s} \frac{\cos(y - y_e - \frac{1}{2}\pi)}{\cos \frac{y-z}{2}}. \quad (96)$$

In this last form we can evaluate $\tan \theta$ safely at the north pole and find $\tan \theta_e = 1/s = \frac{1}{2} \dot{x}_e / \dot{y}_e$. For φ we obtain $\varphi_e = (y_e + z_e)/2 = y_e + \pi/2$.

Note that deriving equation (95) with respect to the affine parameter q and using the equation for \dot{x} in (93) reproduces the equation for \dot{y} in (94), which we may therefore drop.

A.2 Second photon

Equation (95) yields

$$\delta y_e \sim -\epsilon \frac{s f_0}{\sqrt{1 - s^2 f_0^2}} = -\epsilon s f_0 V_0. \quad (97)$$

With

$$W_\epsilon := 2 \left[\frac{1}{a^2} + \frac{\tilde{s}^2}{c^2} \right]^{-1/2} \sim W \left[1 - \frac{\epsilon s^2}{4c^2} W^2 \right], \quad V_\epsilon := [1 - \tilde{s}^2 f^2]^{-1/2} \sim V [1 + \epsilon s^2 f^2 V^2], \quad (98)$$

the two equations (19),(20) yield,

$$\frac{1}{a_0^2} W_0 T_D - \frac{1}{a_e^2} W_e T \sim \epsilon s^2 \left(\frac{1}{4} \int_{t_e}^{t_0} \frac{W^3}{a^2 c^2} + \int_{x_e}^{x_0} f^2 V^3 \right), \quad (99)$$

$$\begin{aligned} \left[\frac{1}{a_0^2} - \frac{1}{c_0^2} \right] W_0 T_D - \left[\frac{1}{a_e^2} - \frac{1}{c_e^2} \right] W_e T &\sim \epsilon \int_{t_e}^{t_0} \left[\frac{1}{a^2} - \frac{1}{c^2} \right] \left(\frac{s^2}{4} \frac{W^3}{c^2} - W \right) - 2\delta \frac{y_e}{s} \\ &\sim -\frac{1}{4}\epsilon \int_{t_e}^{t_0} \left[\frac{1}{a^2} - \frac{1}{c^2} \right] \frac{W^3}{a^2} + 2\epsilon f_0 V_0. \end{aligned} \quad (100)$$

Now we take $(1 + s^2)$ times equation (99) and subtract s^2 times equation (100). We obtain,

$$\begin{aligned}
4 \left(\frac{T_D}{W_0} - \frac{T}{W_e} \right) &\sim \epsilon s^2 \left(\frac{1}{4} \int_{t_e}^{t_0} \left[\frac{1}{a^2} + \frac{s^2}{c^2} \right] \frac{W^3}{a^2} + (1 + s^2) \int_{x_e}^{x_0} f^2 V^3 - 2f_0 V_0 \right) \\
&= \epsilon s^2 \left(\int_{t_e}^{t_0} \frac{W}{a^2} + (1 + s^2) \int_{x_e}^{x_0} f^2 V^3 - 2f_0 V_0 \right) \\
&= \epsilon s^2 \left(\int_{x_e}^{x_0} V + (1 + s^2) \int_{x_e}^{x_0} f^2 V^3 - 2f_0 V_0 \right) \\
&= \epsilon s^2 \left(\int_{x_e}^{x_0} (1 + f^2) V^3 - 2f_0 V_0 \right) = \epsilon s^2 (2fV|_{x_e}^{x_0} - 2f_0 V_0) = 0, \quad (101)
\end{aligned}$$

where we have used successively the definition of W (the second of the four definitions (17)), equation (19), the definition of V (the fourth of the definitions (17)), the second of the two integrals (91) and the first of the limits (92).

B Apparent luminosity

Explicitely the three 3-vectors are:

$$\vec{x}' = \frac{sW}{a^2} \begin{pmatrix} (sV)^{-1} \\ f_x \\ -f_x + \left[1 - \frac{a^2}{c^2} \right] \end{pmatrix}, \quad \vec{\delta} = \delta y_e \begin{pmatrix} 0 \\ 1 \\ 1 \end{pmatrix}, \quad (102)$$

$$\vec{\epsilon} = \epsilon \frac{s^2}{1 + s^2} \left\{ f \begin{pmatrix} -2 \\ (sV)^{-1} \\ -(sV)^{-1} \end{pmatrix} + sI_3 \begin{pmatrix} (sV)^{-1} \\ f_x \\ -f_x + \frac{(1+s^2)}{s^2} \end{pmatrix} \right\}, \quad (103)$$

with

$$I_3(t) := \frac{1}{4} \int_{t_e}^t \frac{W^3}{a^2} \left[\frac{1}{a^2} - \frac{1}{c^2} \right].$$

The derivation of equations (102) is straight-forward. For equation (103) it is convenient to start with equation (19) in the form

$$\int_{t_e}^t \frac{W}{a^2} = \int_{x_e}^x V = \frac{2}{\sqrt{1 + s^2}} \arctan(\sqrt{1 + s^2} f V) =: G(x, s), \quad (104)$$

and to replace $s \rightarrow s(1 + \epsilon)$ and $x \rightarrow x + \epsilon_x$,

$$\int_{t_e}^t \frac{W_\epsilon}{a^2} = G(x + \epsilon_x, s + s\epsilon), \quad (105)$$

with W_ϵ given by the first of equations (98):

$$W_\epsilon \sim W \left[1 - \frac{\epsilon s^2}{4c^2} W^2 \right]. \quad (106)$$

For the linearization we also need,

$$\partial_x G = V, \quad \text{and} \quad \partial_s G = \frac{s}{1+s^2} (2fV - G), \quad (107)$$

and with the algebraic identity,

$$\frac{1}{4} \frac{W^2}{c^2} - \frac{1}{1+s^2} = -\frac{1}{1+s^2} \frac{1}{4} W^2 \left[\frac{1}{a^2} - \frac{1}{c^2} \right], \quad (108)$$

we obtain the x -component of $\vec{\epsilon}$ in equation (103). The y - and z -components then are computed by linearizing the third of equations (18), $\sin(y - y_e) = sf(x)$, and equation (20).

Let us denote by $\vec{\delta} \cdot \vec{\epsilon}$ the negative of the scalar product of 3-vectors defined by the spatial part of the metric tensor $g_{\mu\nu}$ in equation (2). In particular $\vec{x}' \cdot \vec{x}' = 1$, since we have set the speed of light to one. For the other five scalar products we find:

$$\begin{aligned} \vec{\delta} \cdot \vec{x}' &= 0, \quad \vec{\epsilon} \cdot \vec{x}' = 0, \quad \vec{\delta} \cdot \vec{\delta} = \frac{1}{4} \delta^2 y_e^2 \cos^2 x [a^2 + c^2 f^2], \\ \vec{\epsilon} \cdot \vec{\epsilon} &= \frac{\epsilon^2 s^2}{(1+s^2)^2} \left\{ s^2 a^2 f^2 + \frac{1}{4} [a^2 f^2 + c^2] \frac{\cos^2 x}{V^2} \right. \\ &\quad \left. - 2I_3 \frac{a^2 c^2}{W^2} \frac{\cos x}{V} + I_3^2 \frac{a^2 c^2}{W^2} \right\}, \\ \vec{\delta} \cdot \vec{\epsilon} &= \frac{\delta \epsilon y_e s}{(1+s^2)} \left\{ \frac{1}{4} (a^2 - c^2) \frac{\cos x}{V} + I_3 \frac{a^2 c^2}{W^2} \right\} (1 + \sin x). \end{aligned} \quad (109)$$

C Jacobi elliptic and related functions

The Jacobi elliptic functions $\text{cn}(u, k^2)$, $\text{sn}(u, k^2)$, $\text{dn}(u, k^2)$ with $k^2 \in [0, 1]$ interpolate between trigonometric functions for $k^2 = 0$ and hyperbolic ones for $k^2 = 1$ according to

$$\text{cn}(u, 0) = \cos u, \quad \text{sn}(u, 0) = \sin u, \quad \text{dn}(u, 0) = 1, \quad (110)$$

$$\text{cn}(u, 1) = \tanh u, \quad \text{sn}(u, 1) = 1/\cosh u, \quad \text{dn}(u, 1) = 1/\cosh u. \quad (111)$$

These functions may be defined from the differential system (dropping the second argument, which will always be the fixed number k^2):

$$\frac{d}{du} \text{cn } u = -\text{sn } u \text{ dn } u, \quad \frac{d}{du} \text{sn } u = \text{cn } u \text{ dn } u, \quad \frac{d}{du} \text{dn } u = -k^2 \text{cn } u \text{ sn } u, \quad (112)$$

with the initial conditions: $\text{sn } 0 = 0$, $\text{cn } 0 = 1$, $\text{dn } 0 = 1$. These definitions imply the algebraic relations

$$\text{cn}^2 u + \text{sn}^2 u = 1, \quad \text{dn}^2 u + k^2 \text{sn}^2 u = 1. \quad (113)$$

We will indicate the inverse functions by arc. Of paramount importance are the elliptic integrals K and K' (not a derivative) defined by

$$K(k^2) := \int_0^{\pi/2} \frac{dx}{\sqrt{(1-x^2)(1-k^2x^2)}}, \quad K'(k^2) := K(1-k^2). \quad (114)$$

In fact Jacobi even defined the functions $\text{cn}(u)$, $\text{sn}(u)$ and $\text{dn}(u)$ for complex values of u , revealing that their squares are meromorphic and doubly periodic functions with periods $(2K, 2iK')$. What is special with elliptic functions is that besides their double periodicity they must have either a double pole or two simple poles in their period parallelogram, otherwise they are reduced to a constant.

We also need the first of the four Theta functions and follow the conventions of Whittaker & Watson (1986),

$$\theta_1(v, q) := 2 \sum_{n \geq 0} (-1)^n q^{(n+1/2)^2} \sin((2n+1)v). \quad (115)$$

For the user's convenience table 1 summarizes a few commands accessing Jacobi elliptic functions and others in Mathematica and Maple.

	Mathematica	Maple
$\text{cn}(u, k^2)$	JacobiCN[u,k^2]	JacobiCN(u,k)
$\text{arc cn}(u, k^2)$	InverseJacobiCN[u,k^2]	InverseJacobiCN(u,k)
$K(k^2)$	EllipticK[k^2]	EllipticK(k)
$\theta_i(v, q)$, $i = 1, 2, 3, 4$	EllipticTheta[i, v, q]	JacobiThetai(v,q)

Table 1: A few access commands in Mathematica and Maple. Note the absence of the square on k in Maple. Note also that EllipticTheta[i, v, q] are not elliptic functions.

References

- Aluri P. K., Cea P. et al., 2023, *Class. Quant. Grav.*, 40, 094001
 Belinsky, V. A., Khalatnikov, I. M., Lifshitz, E.M., 1971, *JETP*, 60, 1969
 Belinsky, V. A., Khalatnikov, I. M., Lifshitz, E.M., 1972, *JETP*, 62, 1606
 Berger M., 1961, *Ann. Scuola Norm. Sup. Pisa*, 15, 179
 Betoule M. et al. [SDSS], 2014, *Astron. Astrophys.*, 568, A22
 Bianchi L., 1898, *Memorie di Matematica e di Fisica della Societa Italiana delle Scienze*, 11, 267352; English translation by Jantzen R. T., 2001, *Gen. Rel. Grav.*, 33, 2171
 for Engineers and Scientists, 2nd edition, page 135. Springer-Verlag
 Campanelli L., Cea P., Fogli G. L., Marrone A., 2011, *Phys. Rev. D*, 83, 103503
 Cea P., 2014, *MNRAS*, 441, 1646
 Collins, C. B., Hawking S., 1973, *MNRAS*, 162, 305
 Coquereaux R., Grossmann A., 1982, *Annals Phys.*, 143, 296

- Coquereaux R., 2015, *Class. Quant. Grav.*, 32, 115013
- Darling J., 2014, *MNRAS*, 442, L66
- Dechant, P. P., Lasenby, A. N., Hobson, M. P., 2009, *Phys. Rev. D.*, 79, 043524
- Dechant, P. P., Lasenby, A. N., Hobson, M. P., 2010, *Class. Quant. Grav.*, 27, 185010
- Deng H.K., Wei H., 2018, *European Physical Journal C* 78,1
- Di Valentino, E., Melchiorri, A., Silk, J., 2019, *Nature Astron.* 4, 196
- Edwards D., 1972, *MNRAS*, 159, 51
- Ellis G. F. R., MacCallum M. A., 1969, *Comm. Math. Phys.*, 12, 108
- Farnsworth D. L., 1967, *J. Math. Phys.*, 8, 2315
- Fleury P., 2015, arXiv:1511.03702 [gr-qc]
- Fleury P., Pitrou C., Uzan J. P., 2015, *Phys. Rev. D*, 91, 043511
- Fubini G., 1903, *Annali di Mat. ser. 3*, 8, 54
- Giani, L., Piattella, O. F., Kamenshchik, A. Y., 2022, *JCAP*, 03, 028
- Hawking S., 1969, *MNRAS*, 142, 129
- King A. R., Ellis G. F. R., 1973, *Comm. Math. Phys.*, 31, 209
- King D. H., 1991, *Phys. Rev. D*, 44, 2356
- Note two misprints, the fourth of equations (B8) should read: $y_4 = r \cos \psi \sin \beta$
and (B14) should be: $dl^2 \equiv \frac{1}{4}S^2[(dx^1)^2 + (dx^2)^2 + 2 \cos x^1 dx^2 dx^3 + (dx^3)^2]$.
- Koivisto T., Mota D. F., 2008a, *ApJ*, 679, 1
- Koivisto T., Mota D. F., 2008b, *JCAP*, 0806, 018
- Kolatt T. S., Lahav O., 2001, *MNRAS*, 323, 859
- Lemaître G., 1933, *Annales Soc. Sci. Bruxelles A*, 53, 51; English translation by
MacCallum M. A., 1997, *Gen. Rel. Grav.*, 29, 641
- Li S. Y., Li Y. L., Zhang T., J. Vinko, Regos E., Wang X., Xi G., Zhan H., 2023,
Sci. China Phys. Mech. Astron., 66, 229511
- Liu, L., Hu, L. J., Tang, L., Wu, Y, 2023, arXiv:2309.11334 [astro-ph.CO]
- Lu L., Wang L., Chen X., Rubin D., Perlmutter S., Baade D., Mould J., Vinko J., Regős E.,
Koekemoer A. M., 2022, *Astrophys. J.*, 941, 71
- Luongo O., Muccino M., Colgáin E. Ó., Sheikh-Jabbari M. M., Yin L., 2022,
Phys. Rev. D, 105, 103510
- Marcori O. H., Pitrou C., Uzan J. P., Pereira T. S., 2018, *Phys. Rev. D*, 98, 023517
- Migkas K., Pacaud F., Schellenberger G., Erler J., Nguyen-Dang N. T., Reiprich T. H.,
Ramos-Ceja M. E., Lovisari L., 2021, *Astron. Astrophys.*, 649, A151
- Misner, C. W., 1969, *Phys. Rev. Lett.*, 22, 1071
- Pereira T. S., Pitrou C., 2019, *Phys. Rev. D*, 100, 123534
- Perivolaropoulos L., 2023, arXiv:2305.12819
- Pitrou C., Pereira T. S., Uzan J. P., 2015, *Phys. Rev. D*, 92, 023501
- Pitrou C., Cusin G., Uzan J. P., 2020, *Phys. Rev. D*, 101, 081301
- Rahman, W., Trotta, R., Boruah, S. S., Hudson, M. J., van Dyk, D. A. 2002, *MNRAS*, 515,139
- Saunders P. T., 1969, *MNRAS*, 142, 213
- Schücker T., Tilquin A., Valent G., 2014, *MNRAS*, 444, 2820
- Secrest N. J., von Hausegger S., Rameez M., Mohayaee R., Sarkar S., Colin J., 2021,
Astrophys. J. Lett., 908, L51
- Siewert T. M., Schmidt-Rubart M., Schwarz D. J., 2021, *Astron. Astrophys.*, 653, A9

Terzis P. A., 2013, arXiv:1304.7894 [math.RT]
Titov O., Lambert S., 2013, A&A, 559, A95
Uzan, J. P., Kirchner, U., Ellis, G. F. R., 2003, MNRAS, 344, L65
Valent, G., 2009, Gen. Rel. Grav., 41, 2433
Valent G., Tilquin A., Schücker T., 2022, arXiv:2211.04844 [gr-qc]
Wald, R. M., 1983, Phys. Rev. D, 28, 2118
Whittaker E. T., Watson G. N., 1986, A Course of Modern Analysis, 4th edition, page 464.
Cambridge University Press
Zhao D., Zhou Y., Chang Z., 2019, MNRAS 486, 5679-89